

COMPARISON OF TAYLOR MAPS WITH RADIO FREQUENCY MULTIPOLES IN A THIN LENS 6D TRACKING CODE*

D.R. Brett[†], R.B. Appleby, The University of Manchester, UK / Cockcroft Institute, UK
 J. Barranco, R. Tomás, R. De Maria, CERN, Geneva, Switzerland

Abstract

SixTrack is a general purpose 6D thin lens tracking code used for dynamic aperture studies. In the high luminosity large hadron collider (LHC) upgrade it is proposed that crab cavities are used to enhance the luminosity. In this study, for the current proposed optics, we consider the use of radio frequency multipoles (RFM) and Taylor maps (TM) as methods to simulate crab cavity elements in the lattice.

HIGH LUMINOSITY LARGE HADRON COLLIDER

The LHC is a 27 km synchrotron with a design centre of mass energy of 14 TeV. The purpose of the high luminosity upgrade (HL-LHC) is to upgrade the peak luminosity to $5 \times 10^{34} \text{ cm}^{-2}\text{s}^{-1}$ with luminosity levelling to reach an integrated luminosity of 250 fb^{-1} per year allowing over 12 years to reach 3000 fb^{-1} after the upgrade [1]. This would be a 10 fold increase in the planned first ten year running of the LHC [2].

Local Crab Crossing Scheme

The optics scheme for the HL-LHC upgrade [3][4] requires a large crossing angle at the interaction point (IP) in order to reach a small β^* of approximately 15 cm. This large crossing angle is required to overcome the impact of beam beam interaction [5]. A large crossing angle introduces luminosity loss due to a reduction of the geometric overlap. In order to recover this loss and control the luminosity a crab crossing scheme [6] is proposed at the two low β IPs. In Fig.1 the crab crossing scheme is shown and the layout around the interaction point proposed for the HL-LHC upgrade[4] is shown in Fig.2 with the relative cavity positions. A $\pi/2$ betatron phase advance is required between the crab cavities across the IP. A transverse deflecting kick is applied at the cavities and the bunches rotate up until the IP, from there they rotate back to their original orientation and the transverse kick removed from the bunch by applying a kick of the same phase with voltage dependent upon the optics in the interaction region (IR). Such a crab cavity crossing scheme has never been tried before for a hadron machine. The first such crossing for a lepton machine was in KEK-B machine [7]. The total voltage

required from the cavities before the IP is,

$$V = \frac{c^2 p_0 \tan(\frac{\theta}{2})}{q\omega\sqrt{\beta^*}\beta_{crab} \sin(\Delta\phi_\beta)}, \quad (1)$$

where p_0 , θ , β_{crab} , ω , ϕ_β are the reference momentum, crossing angle, beta function at the crab cavity, cavity frequency and betatron phase advance between the cavity and IP respectively. In order to reduce the cavity voltage required the crab cavities are installed where β_{crab} is large and respect the phase advance constraints, making the rest of the machine sensitive to the dynamics of the cavities [8].

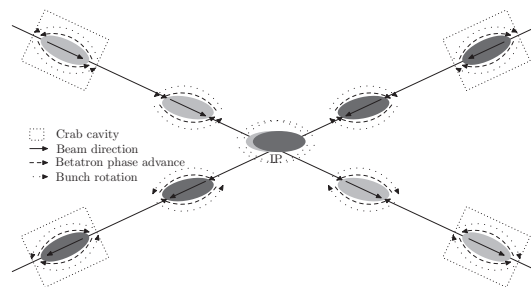


Figure 1: Local crab cavity crossing scheme.

CAVITY MODELS

Two different methods are used to simulate the cavity dynamics, RF multipoles (RFM) [9] and Taylor maps (TM). The RFM method is an extension of the simple kick Hamiltonian in which Fourier decomposed integrated kick coefficients are calculated from the eigenmode solution of a cavity design. The Hamiltonian describing the kick is given by,

$$H = \frac{c}{\omega} \frac{qV_{acc}}{p_0} \sin\left(\frac{\omega z}{c} + \Phi\right) - \sum_{n=1}^N \Re \left[\left(B_n \sin\left(\frac{\omega z}{c} + \Phi\right) + iA_n \sin\left(\frac{\omega z}{c} + \Phi\right) \right) (x + iy)^n \right], \quad (2)$$

where A_n , B_n , V_{acc} , Φ , x , y , z are the skew and normal multipole coefficients, on axis accelerating voltage, phase, transverse positions and canonical longitudinal position relative to the reference particle respectively.

The RFM approximation neglects the orbit variations inside a cavity, the error is small in normalised coordinates for small divergence and low magnitude of the kick compared to the energy of the beam. The validity of this assumption can be seen in Fig.3 [13] for one of the cavity designs, which shows the trajectories of protons in the cavity

* Research supported by EU FP7 HiLumi LHC - Grant Agreement 284404

[†] davebrett@hep.manchester.ac.uk

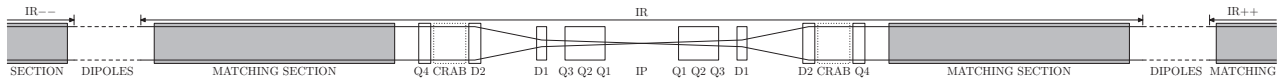


Figure 2: Schematic layout of one low-beta interaction region (IR) proposed for the HL-LHC upgrade with crab cavities showing quadrupoles (Q), dipoles (D) and the corresponding matching sections spread to the IRs either side of low β IR [4].

for the 4 rod design. It is assumed that the radial dependence of the multipolar kicks takes the form of r^n , where n is the order of the multipole, whereas a Bessel-function-like dependence is more appropriate, however, the impact of this is small at small radii.

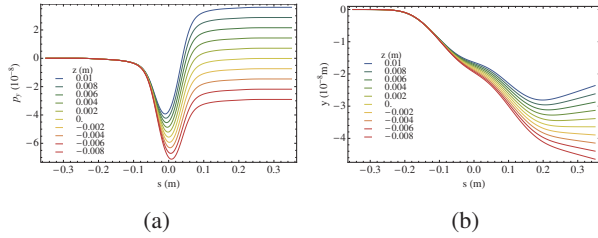


Figure 3: Trajectories through vertically orientated 4 rod cavity design [10]. (a) p_y as a function of s for varying z showing multiple kicks and (b) y as a function of s for varying z showing multiple kicks leading to offset for zero total kick z [13].

In order to develop a more accurate model a second method of simulating the cavities is proposed, using transfer maps expressed as Taylor maps (TM). Such an approach has shown great success for magnetostatic machine elements [11] and has been extended to RF cavities in [12]. The TM are created by symplectically integrating the Hamiltonian of a particle in a vector potential,

$$H = \frac{\delta}{\beta_0} - a_z + p_s - \sqrt{\left(\frac{1}{\beta_0} + \delta\right)^2 - (p_x - a_x)^2 - (p_y - a_y)^2} - \frac{1}{\beta_0^2 \gamma_0^2} \quad (3)$$

where β_0 , \vec{a} , \vec{p}_\perp , γ_0 , p_s , δ is the reference speed as a fraction of c , normalised vector potential, canonical transverse momentum, reference γ , momentum conjugate of position s and conjugate energy deviation, respectively. The Hamiltonian is approximated paraxially and a second order explicit symplectic integration is carried out [14]. The numerical integration is performed using a parallel differential algebra code to 10th order. In order to perform this integration the vector potential is required to be expressed as a Taylor series in x and y as a function of s .

The use of Taylor maps introduces a symplectic error above that of the normal numerical noise from the truncation of the Taylor series. The Jacobian J is said to be symplectic if

$$J^{-1}SJ = S, \quad (4)$$

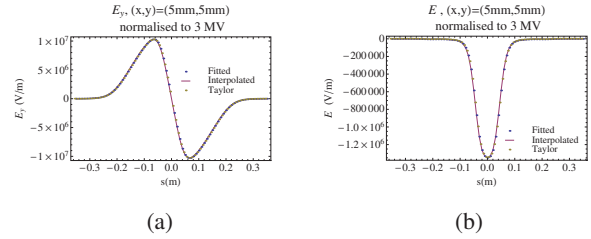


Figure 4: Fitted E fields expressed as harmonic functions (Fitted), Taylor series (Taylor) compared with linearly interpolated meshed data (Interpolated) for vertically orientated 4 rod cavity. (a) Fitted E_y and (b) fitted E_z component of the field.

where S is defined by,

$$S = \begin{pmatrix} 0 & 1 & 0 & 0 & 0 & 0 \\ -1 & 0 & 0 & 0 & 0 & 0 \\ 0 & 0 & 0 & 1 & 0 & 0 \\ 0 & 0 & -1 & 0 & 0 & 0 \\ 0 & 0 & 0 & 0 & 0 & 1 \\ 0 & 0 & 0 & 0 & -1 & 0 \end{pmatrix}. \quad (5)$$

The error matrix E is defined,

$$E = J^{-1}SJ - S, \quad (6)$$

and the terms of this are evaluated at $(x, p_x, y, p_y, z, \delta) = 0.001$ and shown for varying orders of truncation of power series in Fig.5.

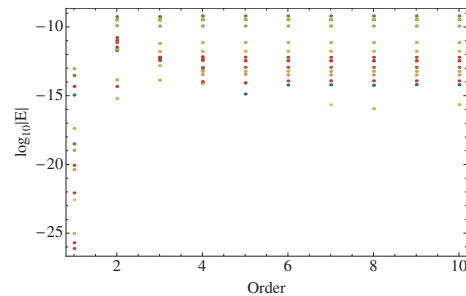


Figure 5: Symplectic error evaluated at $(x, p_x, y, p_y, z, \delta) = 0.001$ for varying order, where the colours are for each of the 36 components of the error matrix (4 rod cavity, normalised to 4.155 MV deflecting kick).

Comparing the Taylor series expanded terms in x , y and z of the RFM method kick, from the momentum change derived from Eq.2, with those of the TM method for the transverse momentum kick it would be expected that these be very similar. This assumes that the trajectory through the cavity is effectively rigid and that the radial dependence

is dominated by the r^n term. In Tab.1 the differences are expressed as a percentage of the total kick ($\Delta p_y = 4.59 \times 10^{-8}$), it can be seen that the greatest magnitude of error at the evaluated position is $5 \times 10^{-2}\%$ for a B_5 term, however at lower radii lower order terms dominate the difference. The difference in B_5 is consistent with contributions from the Bessel like radial dependence of lower order multipoles which is included in the TM and not RFM.

Table 1: Comparison of coefficients from Taylor map and RF multipole kicks for the 4 rod cavity, where the exponents are the 6 powers to which $(x, p_x, y, p_y, z, \delta)$ are raised respectively and n is the order of the term. The difference is evaluated as a percentage of the total kick at $(x, y, z) = 0.01$ m, with units of m and rad for position and momentum variables respectively. Cavity normalised to 3.81933 MV deflecting kick.

Multipole term	Exponent	Terms in Taylor series of p_y		Difference as % of kick
		RFM (rad/m ⁿ)	TM (rad/m ⁿ)	
B_1	000010	4.574×10^{-6}	4.574×10^{-6}	2.18×10^{-4}
	000030	-5.350×10^{-5}	-5.335×10^{-5}	3.37×10^{-4}
B_3	200010	1.235×10^{-4}	1.225×10^{-4}	2.07×10^{-3}
	002010	-1.235×10^{-4}	-1.232×10^{-4}	4.44×10^{-4}
	200030	-1.444×10^{-4}	-1.433×10^{-4}	2.42×10^{-7}
	002030	1.444×10^{-4}	1.442×10^{-4}	5.21×10^{-8}
B_5	202010	3.348	2.009	2.92×10^{-2}
	202030	-3.917×10^1	-2.350×10^1	3.41×10^{-4}
	400010	-5.58×10^{-1}	-3.34×10^{-1}	4.86×10^{-2}
	400030	6.527	3.918	5.68×10^{-5}
	004010	-5.580×10^{-1}	-3.350×10^{-1}	4.86×10^{-2}
	004030	6.527	3.918	5.68×10^{-5}

SixTrack uses a thin lens tracking particle tracking model [15], where thick lens elements are split into a series of momentum kicks and drifts. In order to implement the TMs in the code a new Sixtrack element type anti drift is required. This element removes the drift component on either side of the TM in the tracking code and maintains the correct length for the Sixtrack crab element and is shown in Fig.6. In order to allow for tracking to occur within a reasonable amount of computational time the number of coefficients are reduced through a ranked weighting method based upon their contribution to the dynamics.

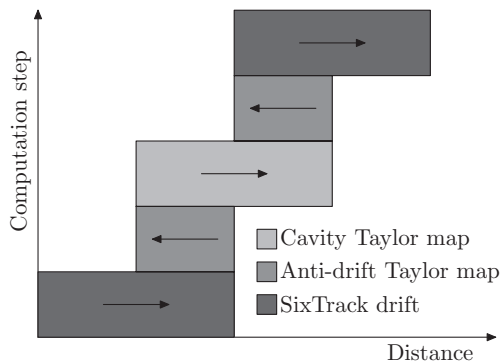


Figure 6: Implementation of Taylor maps in the thin lens tracking code SixTrack.

CONCLUSION

Two methods for simulating crab cavities in the HL-LHC have been developed and implemented into the SixTrack tracking code for dynamic aperture studies. A new implementation of Taylor maps is used in a thin lens tracking regime and the errors and assumptions associated with both methods are presented.

ACKNOWLEDGEMENT

The authors would like to thank Dan Abell and Andy Wolski for helpful discussions on field fitting and integration techniques, Rama Calaga for helpful discussions on crab cavities and Frank Schmidt for helpful clarifications on SixTrack.

REFERENCES

- [1] L Rossi. LHC Upgrade Plans: Options and Strategy TUYA02,IPAC11 Proc., Spain, 2011.
- [2] HiLumi LHC collaboration. FP7 High Luminosity Large Hadron Collider Design Study. FP7-INFRASTRUCTURES-2011-1, pages 1–100, 2011.
- [3] S Fartoukh. Layout and Optics Solutions for the LHC Insertion Upgrade Phase I. IPAC10 Proc., Japan , 2010.
- [4] S Fartoukh. An Achromatic Telescopic Squeezing (ATS) Scheme For The LHC Upgrade. IPAC11 Proc., Spain, 2011.
- [5] A Piwinski. Space charge effect with crossing angle. *NIM*, **81**(1):199-200,1970.
- [6] K Oide and K Yokoya. The crab crossing scheme for storage ring colliders. *Phys. Rev. A* **40**:315, 1989.
- [7] K Nakanishi, Y Funakoshi, and M Tobiyama. Beam behaviour due to crab cavity breakdown. IPAC10 Proc., Japan , 2012.
- [8] Y Sun, R Assmann, J Barranco, and R Tomás. Beam dynamics aspects of crab cavities in the CERN Large Hadron Collider. *Phy. Rev. ST-AB*, 2009.
- [9] J.B García, R. Calaga, R. De Maria, M. Giovannozzi, A. Grudiev, and R. Tomás. Study of Multipolar RF Kicks from the main deflecting mode in Compact Crab Cavities for LHC. IPAC12 Proc., USA, 2012.
- [10] B Hall, G Burt, J Smith, R Rimmer, and H Wang. Novel geometries for the LHC crab cavity. IPAC10 Proc., Japan , 2010.
- [11] M. Venturini and A. Dragt. Accurate computation of transfer maps from magnetic field data. *NIMA*, **427**(1):387–392, 1999.
- [12] D. Abell. Numerical computation of high-order transfer maps for rf cavities. *Phys. Rev. ST Accel. Beams* **9**(5):052001, 2006.
- [13] D.R. Brett, R.B. Appleby, G. Burt, and B. Hall. Particle trajectories in a 4 rod crab cavity. *NIMA*, 2012.
- [14] Y Wu, E Forest, and D Robin. Explicit symplectic integrator for s-dependent static magnetic field. *Phys. Rev. E*, **68**(4):046502, 2003.
- [15] K Heinemann, G Ripken, and F Schmidt. Construction of nonlinear symplectic six-dimensional thin-lens maps by exponentiation. *DESY-95-189*, 1995.